Influence of magnetite stoichiometry on the binding of emerging organic contaminants

Wei Cheng, Remi Marsac, Khalil Hanna

▶ **To cite this version:**

Wei Cheng, Remi Marsac, Khalil Hanna. Influence of magnetite stoichiometry on the binding of emerging organic contaminants. Environmental Science and Technology, 2018, 52 (2), pp.467-473. 10.1021/acs.est.7b04849 . insu-01662350

HAL Id: insu-01662350

https://insu.hal.science/insu-01662350

Submitted on 13 Dec 2017

HAL is a multi-disciplinary open access archive for the deposit and dissemination of scientific research documents, whether they are published or not. The documents may come from teaching and research institutions in France or abroad, or from public or private research centers.

L'archive ouverte pluridisciplinaire **HAL**, est destinée au dépôt et à la diffusion de documents scientifiques de niveau recherche, publiés ou non, émanant des établissements d'enseignement et de recherche français ou étrangers, des laboratoires publics ou privés.

Subscriber access provided by SCD Université de Rennes1 | SCD de l'Université de Rennes 1

Article

Influence of magnetite stoichiometry on the binding of emerging organic contaminants

Wei Cheng, Rémi Marsac, and Khalil Hanna

Environ. Sci. Technol., **Just Accepted Manuscript** • DOI: 10.1021/acs.est.7b04849 • Publication Date (Web): 07 Dec 2017

Downloaded from http://pubs.acs.org on December 13, 2017

Just Accepted

"Just Accepted" manuscripts have been peer-reviewed and accepted for publication. They are posted online prior to technical editing, formatting for publication and author proofing. The American Chemical Society provides "Just Accepted" as a free service to the research community to expedite the dissemination of scientific material as soon as possible after acceptance. "Just Accepted" manuscripts appear in full in PDF format accompanied by an HTML abstract. "Just Accepted" manuscripts have been fully peer reviewed, but should not be considered the official version of record. They are accessible to all readers and citable by the Digital Object Identifier (DOI®). "Just Accepted" is an optional service offered to authors. Therefore, the "Just Accepted" Web site may not include all articles that will be published in the journal. After a manuscript is technically edited and formatted, it will be removed from the "Just Accepted" Web site and published as an ASAP article. Note that technical editing may introduce minor changes to the manuscript text and/or graphics which could affect content, and all legal disclaimers and ethical guidelines that apply to the journal pertain. ACS cannot be held responsible for errors or consequences arising from the use of information contained in these "Just Accepted" manuscripts.

ACS Publications

Environmental Science & Technology is published by the American Chemical Society. 1155 Sixteenth Street N.W., Washington, DC 20036

Published by American Chemical Society. Copyright © American Chemical Society. However, no copyright claim is made to original U.S. Government works, or works produced by employees of any Commonwealth realm Crown government in the course of their duties.

Influence of magnetite stoichiometry on the binding of emerging organic contaminants

Wei Cheng[a], Rémi Marsac [a,b], Khalil Hanna[*a]

[a]École Nationale Supérieure de Chimie de Rennes, UMR CNRS 6226, 11 Allée de Beaulieu, 35708 Rennes Cedex 7, France

[b]Géosciences Rennes, UMR 6118 CNRS – Université Rennes 1, Campus de Beaulieu, 35042 Rennes Cedex, France

*Corresponding author: Tel.: +33 2 23 23 80 27; fax: +33 2 23 23 81 20.

E-mail address: khalil.hanna@ensc-rennes.fr (K. Hanna)

A revised manuscript for ES&T

December 2017

Abstract

While the magnetite stoichiometry (*i.e.* Fe(II)/Fe(III) ratio) has been extensively studied for the reductive transformation of chlorinated or nitroaromatic compounds, no work exists examining the influence of stoichiometry of magnetite on its binding properties. This study, for the first time, demonstrates that the stoichiometry strongly affects the capacity of magnetite to bind not only quinolone antibiotics such as nalidixic acid (NA) and Flumequine (FLU), but also salicylic acid (SA), natural organic matter (humic acid, HA) and dissolved silicates. Fe(II)-amendment of non-stoichiometric magnetite (Fe(II)/Fe(III) = 0.40) led to similar sorbed amounts of NA, FLU, SA, silicates or HA as compared to the stoichiometric magnetite (i.e. Fe(II)/Fe(III) = 0.50). At any pH between 6 and 10, all magnetites exhibiting similar Fe(II)/Fe(III) ratio in the solid phase showed similar adsorption properties for NA or FLU. This enhancement in binding capability of magnetite for NA is still observed in presence of environmentally relevant ligands (e.g. 10 mg L^{-1} of HA or 100 μM of silicates). Using surface complexation modeling, it was shown that the NA-magnetite complexation constant does not vary with Fe(II)/Fe(III) between 0.24 and 0.40, but increases by 8 orders of magnitude when Fe(II)/Fe(III) increases from 0.40 to 0.50.

I. Introduction

Magnetite is an ubiquitous mixed Fe(II)–Fe(III) oxide in soils and sediments, and is very efficient in environmental remediation owing to its reduction capacity.[1,2] For this reason, the reactivity of magnetite to reduce various organic[3–7] and inorganic contaminants[8–11] has been extensively studied. The stoichiometry of the particles (*i.e.* Fe(II)/Fe(III) ratio that can vary from 0 to 0.5) is one of the most important factors in the reduction reaction, and could govern the reactivity of magnetite in natural systems.[6,10,11] Exposing non-stoichiometric magnetite (i.e. low Fe(II)/Fe(III) ratio) to a source of Fe(II) can restore the 0.5 ratio (i.e. perfectly stoichiometric magnetite) through oxidation of adsorbed Fe(II), accompanied by reduction of the octahedral Fe(III) in the underlying magnetite to octahedral Fe(II).[5,6] Therefore, investigations to recharge magnetite surfaces by Fe(II) in order to enhance its reactivity as well as the effect of magnetite stoichiometry on the reduction of contaminants have attracted great attention.[4–7] However, very little is known about the impact of Fe(II)-recharge on adsorption properties of the magnetite surface. Although the magnetite adsorption capacity was evaluated for different compounds including heavy metals and radionuclides,[2,12,13] oxyanions[14,15] and organic ligands,[16] none has attempted to assess the influence of Fe(II)/Fe(III) ratio on the mechanism and extent of binding of these compounds on magnetite surfaces.

In this work, we elucidate these effects in different magnetite suspensions containing Nalidixic Acid (NA) or Flumequine (FLU) (see their structures and speciation in Fig. S1). Because of their growing use in human and veterinary medicine and continuous release into the environment, quinolone antibiotics such as NA and FLU have been detected in surface waters, groundwaters and sediments at concentrations levels ranging from ng L^{-1} to µg L^{-1}.[17–19] As the mobility of these compounds in the environment can be strongly affected by interactions with surfaces of soil and sediment mineral particles[18–19], a thorough

understanding of their sorption behavior is essential. Magnetite and more generally iron (oxy)(hydr)oxides represent important reactive surfaces towards organic ligands in soils and sediments.

Here, we examined both ligand adsorption and Fe(II) dissolution as a function of pH for magnetites exhibiting different Fe(II)/Fe(III) ratio, prepared as such, or through Fe(II) recharge of non-stoichiometric magnetite suspensions. The binding capability of magnetite with respect to Fe(II)/Fe(III) ratio was also examined in presence of naturally occurring ligands (e.g. salicylic acid (SA), silicates and humic acid (HA)). Implication of ternary surface complexation (i.e. surface-metal-ligand complex) in enhancement in ligand adsorption was assessed by investigating the impact of other divalent cations (Mn(II), Ni(II)) on NA adsorption, where metal binding with no electron transfer is supposed to occur on magnetite. We then used surface complexation modeling to describe the observed behavior, and to gain further insights into the mechanisms responsible for enhancing ligand sorption upon Fe(II)-recharge. The present work notably revealed a considerable impact of the magnetite stoichiometry on the sorption capability of magnetite surfaces.

II. Experimental

Chemicals. If not mentioned, chemicals (all pro analytical quality or better) were obtained from Sigma Aldrich. Leonardite Humic Acid standard (LHA) was purchased from the International Humic Substances Society (IHSS). Solutions were prepared with ultrapure "MilliQ" water (specific resistivity, 18.2 MΩ cm^{-1}) purged with N_2 for 4 h. Magnetite (ideal formula: Fe_3O_4) was synthesized applying a procedure involving a room temperature aqueous precipitation method in an anaerobic chamber (JACOMEX). A 0.3 M HCl solution containing a $FeCl_2$:$FeCl_3$ 1:2 molar ratio was introduced into an N_2-sparged 25% w/v ammonium (NH_4OH) solution, with continuous stirring at 1400 rpm, leading to instantaneous

84 precipitation of magnetite particles. Because washing steps can lead to the loss of Fe(II),[6] no
85 washing step was applied to obtain the stoichiometric magnetite (M0.50; the number refers to
86 Fe(II)/Fe(III) ratio). The solid concentration was 25 g L^{-1} (5g in 200 mL) and the pH was 8.3.
87 Other magnetites, Fe(II)-depleted, were obtained from M0.50. By applying one washing step
88 to a fraction of M0.50 suspension with N_2-purged ultrapure water and then centrifuged for 5
89 min at 4000 rpm, M0.44 was obtained. By applying three washing steps to M0.50, M0.40 or
90 M0.42 can be obtained. By exposing the M0.50 during 24h to a known amount of H_2O_2
91 (following the procedure of Gorski et al.[6]), M0.42 (denoted as M0.42-H_2O_2) and M0.33 were
92 obtained. By exposing the M0.50 during 24h to ambient air, M0.24 was obtained.

93 **Characterization of magnetite particles.** The mineral identify was confirmed by X-ray
94 diffraction (see XRD pattern in Fig. S2). According to TEM micrographs (Fig. S2), the
95 synthetic magnetite particles are 10 to 15 nm in diameter (12.5 nm on average). Similar XRD
96 patterns were found for the different magnetites investigated here, and no notable influence of
97 the stoichiometry of the particles on particle size was observed. Accordingly, B.E.T. surface
98 area did not significantly differ between the magnetites used in this study (89 ± 4 m^2 g^{-1}).
99 Using the assumption that all magnetite particles are spherical in shape (density = 5.15 x10^6 g
100 m^{-3})[1], TEM surface area was determined to be 93 m^2 $g^{-1,}$ close to the BET one.

101 An aliquot of each magnetite suspension was taken and digested in N_2-sparged 5 M HCl
102 inside the glovebox overnight with shaking. Dissolved Fe(II) and Fe(III) concentrations were
103 then determined using the phenanthroline method.[20] This bulk Fe(II) content was found very
104 close to that determined by acid digestion on the filtered solid, as previously reported.[5,6] The
105 amount of magnetite bound-Fe(II) ($[Fe(II)]_{bound} = [Fe(II)]_{tot} - [Fe(II)]_{aq}$) was used to calculate
106 the effective Fe(II)/Fe(III) ratio (denoted as $(Fe(II)/Fe(III))_{bound}$) in magnetite which was
107 shown to vary with pH (see results and discussion section). $[Fe(II)]_{tot}$ is the total concentration

of Fe(II) in the suspension (solid + solution) and $[Fe(II)]_{aq}$ is the dissolved concentration of Fe(II), measured after filtration (0.2 μm, Whatman) of the magnetite suspension.

Adsorption experiments. Adsorption batch experiments were carried out in 15 mL polypropylene tubes under anaerobic conditions (glovebox). NaCl concentration was set to 10 mM for all experiments. The effect of dissolved Fe(II) on NA or FLU adsorption to magnetite was investigated by adding small amounts of 100 mM $FeCl_2$ solution (dissolved in 0.1 M HCl). pH was adjusted using 0.1 M NaOH/HCl solutions. After 24h reaction time, an aliquot was taken and filtered (0.2 μm, Whatman) for high performance liquid chromatography analysis with UV-vis detection (HPLC-UV) and dissolved Fe(II) analysis by the phenanthroline method. Aqueous concentrations of NA or FLU were determined using HPLC (Waters 600 Controller) equipped with a reversed-phase C18 column (250 mm×4.6 mm i.d., 5 μm) and a UV-vis detector (Waters 2489). The mobile phase was mixture of acetonitrile/water (60/40 v/v) contained 0.1% formic acid. The flow rate was set at 1 ml min^{-1} in isocratic mode. The UV detector was set to 258 nm for NA and 246 nm for FLU.

Note that kinetic experiments at pH = 8.5 revealed that (i) NA binding to magnetite (M0.50 or M0.42) and Fe(II) uptake by M0.42 occurred within less than 5 minutes and (ii) the order of adding chemicals (i.e. addition of NA to 24h pre-equilibrated M0.42 with Fe(II) or addition of Fe(II) to 24h pre-equilibrated M0.42 with NA) had no impact on the binding behavior (See Fig. S3). NA adsorption isotherms on M0.50 and M0.42 were also investigated at pH = 7 ($20 \leq [NA] \leq 300$ μM).

The same procedure was applied to test the effect of Mn(II) and Ni(II) on NA adsorption to M0.40. Dissolved Mn(II) and Ni(II) concentrations were determined by Atomic absorption spectroscopy (AAS, Shimadzu). The effect of 10 mg L^{-1} HA or 100 μM silicates on the adsorption of 20 μM NA to magnetite was also investigated, applying the same procedure. HA concentrations in solution were monitored using an organic carbon analyzer (Shimadzu

TOC-VCSH). SA concentration was determined using UV-Visible spectrophotometer at 297 nm. Silicates concentrations were determined by the molybdenum-blue colorimetric method.[21]

Surface complexation modeling. The geochemical speciation code PHREEQC (version 2)[22] and the "minteq" database provided with this code were used. At infinite dilution, the pK_a of NA and FLU equal 6.19 and 6.31, respectively, and the logarithm of the formation constant of NA-$Fe^{+}_{(aq)}$ and FLU-$Fe^{+}_{(aq)}$ equal 3.99 and 4.23, respectively ; as calculated from reported conditional constant values and the Davies equation.[23,24] The surface complexation models developed by Jolsterå et al.[25] for magnetite and maghemite were used to predict NA and FLU adsorption to magnetite with different stoichiometry. Maghemite γ-$Fe^{III}_2O_3$ is considered as an extreme example of a non-stoichiometric magnetite ($Fe^{II}_1Fe^{III}_2O_4$), with only Fe^{III} in both tetrahedral and octahedral sites[1].

Surface site protonation is formulated as follows (2-pKa approach):

$$\equiv FeOH_2^+ \rightleftharpoons \equiv FeOH + H^+ \quad ; pKa_{,1} \qquad (1)$$

$$\equiv FeOH \rightleftharpoons \equiv FeO^- + H^+ \quad ; pKa_{,2} \qquad (2)$$

Charge-potential relationship is described according to the constant capacitance model (CCM). Model parameters for magnetite and maghemite are reported in Table S1. The CCM is not implemented in PHREEQC, but it can be used via a three plane model (TPM; available in PHREEQC), in which one capacitor and the diffuse layer are suppressed, following the procedure detailed in Marsac et al.[26].

III. Results and discussion

Binding capacity *vs* magnetite stoichiometry. Nalidixic acid (NA) adsorption to four magnetites exhibiting different Fe(II)/Fe(III) ratio (0.40, 0.42, 0.44 and 0.50) showed that NA adsorption was strongly related to the stoichiometry of the particles (*i.e.* Fe(II)/Fe(III) ratio vary from 0.40 for non-stoichiometric magnetite, to 0.50 for stoichiometric magnetite; Fig.

158 1a). NA adsorption to M0.40 decreased with increasing pH, as typically encountered for
159 anionic ligands, and became negligible for pH > 7.5. Indeed, adsorption of anionic ligands to
160 mineral oxides is typically greatest under acidic to circumneutral pH, and lowest under
161 alkaline conditions, with maximum adsorption generally observed at a pH near the pK_a (i.e.
162 6.19 for NA).[27–31] At higher stoichiometry (0.42, 0.44 or 0.50), pH dependence of NA
163 sorption was significantly altered. NA adsorption increased from pH 6 to 7 < pH < 8 and then
164 decreased with increasing pH, thereby shifting the maximum NA adsorption to larger pH
165 values than the pK_a. Note that adsorption of NA to M0.42 prepared either by washing or
166 oxidizing (H_2O_2) of M0.50 was similar. The data are merged in Fig. 1a (see Fig. S4 for more
167 details).

168 Fe(II)-amendement of non-stoichiometric magnetite (M0.40 and M0.42) led also to an
169 enhancement in NA adsorption (Fig. 1a). Indeed, the pH-adsorption curve of NA shifted to
170 larger pH values with increasing added amounts of dissolved Fe(II), a result suggesting that
171 NA binding was closely related to the Fe(II) content or Fe(II)/Fe(III) ratio in magnetite. The
172 Fe(II) recharge of non-stoichiometric magnetite provided the same adsorption capability as
173 for the corresponding magnetite with higher stoichiometry on the whole pH-range
174 investigated (i.e. Fe(II)/Fe(III) = 0.42 for M0.40 + 100 µM Fe(II) and M0.42 ; Fe(II)/Fe(III) =
175 0.44 for M0.40 + 200µM Fe(II) and M0.44 ; Fe(II)/Fe(III) = 0.50 for M0.40 + 500µM Fe(II),
176 M0.42 + 400 µM Fe(II) and M0.50).

177 Because of Fe(II) dissolution, the amount of bound-Fe(II) in magnetite can vary
178 depending on pH, which may affect the NA adsorption. Indeed, $[Fe(II)]_{aq}$ increased with
179 decreasing pH (no dissolved Fe(III) was found), due to the H^+ promoted dissolution of
180 magnetite,[32,33] but also with magnetite stoichiometry (i.e. M0.40 < M0.44 < M0.50) (Figure
181 1b). Exposing a non-stoichiometric magnetite (M0.40) to 200 or 500 µM Fe(II) led to similar
182 Fe(II) aqueous concentration as those measured with M0.44 or M0.50, respectively. Note that

only up to ~10% of magnetite could dissolve in our experiments (*e.g.* for M0.50 at the lowest pH investigated, *i.e.* 6). Therefore, the effect of magnetite dissolution on NA adsorption can be neglected.

As expected, $(Fe(II)/Fe(III))_{bound}$ increased with Fe(II)-recharge of non-stoichiometric magnetite and pH (Figure 1c). Variation in $(Fe(II)/Fe(III))_{bound}$ appeared fully consistent with the magnetite ability to bind NA. For instance, all magnetites exhibiting similar $(Fe(II)/Fe(III))_{bound}$ values showed similar NA sorbed amounts whatever the investigated pH, though the dissolved Fe(II) amounts are different (especially at low pH values < 7.5) (Fig. 1b). For instance, M0.50 shows the same binding capability for NA as for the corresponding Fe(II)-amended magnetite (i.e. M0.40 + 500 µM Fe(II) and M0.42 + 400 µM Fe(II)), and therefore similar surface properties with respect to NA adsorption. This is also true for M0.40 + 200 µM Fe(II) *vs* M0.44, and further illustrated in Fig. S5, where variations of NA sorbed amounts at pH 7.7 as a function of $(Fe(II)/Fe(III))_{bound}$ followed the same trend for both stoichiometric magnetite (M0.5) and Fe(II)-amended non-stoichiometric magnetites (M0.40 and M0.44). Likewise, enhancement in Flumequine (FLU) adsorption was observed with increasing amounts of added Fe(II) to M0.40 or $(Fe(II)/Fe(III))_{bound}$ (Fig. S6). Desorption tests were conducted by adjusting pH to 11 after the system has reached equilibrium and then stirred for around 2 h. Mass balance showed that NA or FLU was removed only by adsorption and that transformation by, for example, reduction, did not occur under the experimental conditions of this study.

Formation of ternary surface complexes (i.e. surface-metal-ligand complex) generally entails more ligand adsorption when complexing cation concentration increases [34], which might explain the enhancement in NA or FLU binding to magnetite. To test this hypothesis, impacts of presence of two divalent cations (Mn(II) and Ni(II)) on NA adsorption to M0.40 were investigated and compared with that of Fe(II). Because the redox potential of the

208 $Mn^{II}/MnO_{2(s)}$ couple at pH = 7 is much larger than that of $Fe^{II}/Fe_3O_{4(s)}$, Mn(II) oxidation by
209 magnetite is not expected.[35] According to the Irving-Williams series,[36] cation adsorption
210 data[35] and aqueous complexation with NA,[23,37] ternary surface complexation of Mn(II), Fe(II)
211 and Ni(II) with NA on magnetite are supposed to follow the order: Mn(II) < Fe(II) < Ni(II)[34]
212 (assuming that no electron transfer occurs between Fe(II) and the solid). This ranking is,
213 however, observed neither for metal uptake nor for NA adsorption to M0.40 (Fig. 2). Indeed,
214 more Fe(II) uptake than Ni(II) is achieved (Fig. 2a), whereas maximum NA adsorption was
215 obtained at pH ≈ 7.5 for Fe(II) and pH ≈ 8.5 for Mn(II) and Ni(II). This observation is also
216 confirmed at higher metal concentration (e.g. 500μM, Fig. S7), thereby underscoring a
217 different adsorption behavior of NA in presence of Fe(II) with respect to other divalent
218 transition metals.

219 Taken together, these findings suggest that the adsorption enhancement for NA is mainly
220 controlled by the $(Fe(II)/Fe(III))_{bound}$ ratio in magnetite, rather than by NA-Fe(II)
221 complexation in solution at low pH or ternary surface complexation. As a matter of fact, the
222 enhanced binding of ligands to stoichiometric magnetite with respect to non-stoichiometric
223 one may result from the creation of new binding sites upon Fe(II)-recharge, or changes in the
224 intrinsic surface reactivity of amended magnetite.

225

226 **Description of enhancement sorption capacity.** As an attempt to describe the
227 relationship between $(Fe(II)/Fe(III))_{bound}$ and ligand adsorption, we used a surface
228 complexation modeling approach. The aim of the present modeling exercise was to provide a
229 semi-quantitative evaluation of how much magnetite surface reactivity towards quinolones is
230 affected by its stoichiometry. Because of the possible presence of various types of
231 $\equiv Fe^{II/III}O(H)$ groups at magnetite surfaces, full mechanistic description of binding
232 mechanisms using a complete approach would have required fitting of many parameters, and

then generated large errors on simulated phenomena. Therefore, we used the 2-pKa-CCM approach developed by Jolsterå et al.[25]. Using acid-base titration method, they have calculated site densities of 1.50 nm^{-2} and 0.99 nm^{-2} for magnetite (91 $m^2\ g^{-1}$) and maghemite (86 $m^2\ g^{-1}$), respectively

As shown in Figure S8, fitting experimental adsorption isotherms of NA on M0.50 and M0.42 at pH = 7 with Langmuir equation results in a maximum binding capacity of 0.95 and 0.71 NA molecule nm^{-2}, respectively. Previous studies on quinolones binding to iron (hydr)oxides evidenced that one molecule binds to two surface hydroxo groups,[29,38,39] by involving its carboxylate and its keto-group as following:

$$2\ \equiv FeOH + 2\ H^+ + NA^- \rightleftharpoons (\equiv Fe)_2NA^+ + 2\ H_2O \qquad {}^{S}K$$

Hence, the maximum binding of NA to magnetites corresponds to 1.90 to 1.42 site nm^{-2}, which are relatively close to those determined by Jolsterå et al.[25]. As the present modeling exercise aimed to determine surface complexation constant (^{S}K) to each magnetite, we focused only on the pH-edge curve (obtained at low surface coverage) and thus used the same site density for all magnetites (1.50 nm^{-2}). Measured total dissolved Fe(II) concentration in solution at the end of each adsorption experiment was used as input parameter to account for ligand-Fe(II) complexation in solution. However, decreasing ligand adsorption with decreasing pH (i.e. at high $[Fe(II)]_{aq}$) could not be well predicted, further suggesting that effects of variation of $(Fe(II)/Fe(III))_{bound}$ were more important than the ligand-Fe(II) aqueous complexation. Therefore, we only focused on data at high pH values, where $(Fe(II)/Fe(III))_{bound}$ is maximal and constant (see Fig. 1c; e.g. pH > 8 for M0.50, pH > 6.5 for M0.40). As shown in Figure 1a (NA) and Figure S6 (FLU), a relatively good fit to the adsorption data versus pH was found (unsuccessful extrapolations at lower pH are shown as dotted lines in Fig. 1a and S6). When plotting log ^{S}K for NA versus $(Fe(II)/Fe(III))_{bound}$ (Fig.

3), a linear relationship was found (R^2=0.99). Data for FLU are also included and show a comparable behavior. Values of log ^{S}K increased by almost 8 orders of magnitude with increasing $(Fe(II)/Fe(III))_{bound}$ from 0.40 to 0.50, suggesting that stoichiometric magnetite (Fe(II)-enriched) may have a much stronger affinity for NA or FLU than partially oxidized magnetite (Fe(II)-depleted). Such large variation in log ^{S}K cannot be attributed to potential modification in surface site density that was neglected by using the same site density for all magnetites. As more amount of Fe(II) at the magnetite surface is expected upon Fe(II) recharge, we may suppose that $\equiv Fe^{II}O(H)$ sites are more reactive than $\equiv Fe^{III}O(H)$ for NA or FLU binding.

To test the binding capacity of magnetite with lower stoichiometries, we prepared M0.33 and M0.24 (similar to magnetites found in some natural samples[40,41]), by exposing the M0.50 during 24h to (i) a known amount of H_2O_2 (following the procedure of Gorski et al.[6]) and (ii) ambient air, respectively. Both oxidized magnetites exhibited similar NA adsorption, whereas $[Fe(II)]_{aq}$ were found very low (Fig. 1b). For pH $\leq$ 7, more pronounced NA adsorption was observed on M0.33 and M0.24 as compared to M0.40, a result that can be attributed to the complete suppression of dissolved Fe(II) at low pH. Consistently, the best fitting values of ^{S}K were found very close for M0.24, M0.33 (log ^{S}K = 17.7) and M0.40 (log ^{S}K = 17.5). It is worth noting that the calculated surface complexation constant ^{S}K remains constant for $0.23 < (Fe(II)/Fe(III))_{bound} < 0.40$, and then sharply increased after 0.40 (Fig. 2). The existence of a threshold may be related to the surface amount of magnetite bound-Fe(II) required to trigger the enhancement of NA binding with magnetite surfaces.

Because non-stoichiometric magnetites may have oxidized magnetite/maghemite-like structure at the outermost surface (oxidation of magnetite particles is supposed to take place from the surface to the core [25]), NA adsorption to magnetites with Fe(II)/Fe(III) $\leq$ 0.42 was also evaluated using the surface complexation model developed for maghemite (i.e. fully

oxidized magnetite). Because of the little variation in site density, surface area and acid-base properties, log ^{S}K (for NA and FLU) determined using magnetite model or maghemite model were found very similar (Fig. 4).

This modification in binding properties is not specifically limited to NA or FLU molecule, since the adsorption of naturally occurring ligands such as salicylate (1-hydroxybenzoic acid, SA), humic acid (HA) and silicates (Si) was also considerably enhanced by the addition of dissolved Fe(II) to a non-stoichiometric magnetite M0.40 (See Figures S9-S11). Consequently, the stoichiometry of magnetite is not only a key parameter for Fe(II) uptake[5] and contaminant reduction[6,10,11] but also for the binding of emerging organic contaminants and naturally occurring ligands. Because emerging contaminants binding to magnetite might be affected by naturally occurring ligands, competitive experiments between NA and HA or Si were conducted. The presence of 100 μM Si decreased NA binding to magnetite due to ligand competition, though the effect of Si on NA adsorption to M0.40 is insignificant (Fig. 4a). However, the impact of 10 mg L^{-1} HA on NA binding implies both competitive (i.e. antagonistic effect) and cooperative (i.e. synergetic effect) mechanisms (Fig. 4b). Indeed, at high Fe(II)/Fe(III), HA effectively decreases NA binding whereas, at low Fe(II)/Fe(III), NA binding is enhanced in presence of HA. The latter may arise from intermolecular interactions between HA and NA, as previously observed between NA and other organic compounds at goethite surfaces,[38,39] and supported by a quinolone-HA binding study.[42] While further investigations are required to understand the different competitive and cooperative effects, this data further supports that (i) binding properties of magnetite is affected upon Fe(II)-recharge, and (ii) this change towards adsorption of emerging contaminants is still observed in presence of naturally occurring ligands.

Environmental implications. Magnetites of differential composition and stoichiometry may exist in natural systems depending on the local redox and chemical

conditions, particularly in Fe-rich subsurface environments or temporary flooded soils (e.g. wetlands experiencing redox potential fluctuation).[1,2,38,39] Given its higher solubility and surface area-to-volume ratio, Fe(II) release and/or surface oxidation may occur for the nanosized magnetite, commonly found in environmental systems[1]. On the other hand, different kinds of magnetite can be obtained depending on the synthesis method, as reported in water remediation studies using magnetite as sorbent.[27,31,32] Consequently, the stoichiometry of magnetite and its potential Fe(II)-enrichment or Fe(II)-depletion in reaction medium should be appropriately considered in sorption and reactive transport studies. It is worth noting that the changes in binding properties of magnetite upon Fe(II)-recharge are still observed in presence of natural ligands, emphasizing the importance of the presently evidenced mechanisms in environmentally relevant conditions. Therefore, these findings call for refinements in current day modeling approaches used in the prediction of fate of organic contaminants in Fe-rich subsurface environments or magnetite-based remediation processes.

Acknowledgements. The authors gratefully acknowledge the financial support of this work by ADEME "Agence de l'Environnement et de la Maîtrise de l'Energie" N° of funding decision 1472C0030.

Supporting Information Available. Characterization data of magnetite particles, NA and FLU aqueous speciation versus pH, surface complexation model parameters, additional results for adsorption kinetics and isotherms, impacts of cationic metals, Si and HA on adsorption behavior. This information is available free of charge via the Internet at http://pubs.acs.org/.

References

(1) Maher, B. A.; Taylor, R. M. Formation of ultrafine-grained magnetite in soils. *Nature* **1988**, *336* (6197), 368–370.

(2) Singer, D. M.; Chatman, S. M.; Ilton, E. S.; Rosso, K. M.; Banfield, J. F.; Waychunas, G. A. U(VI) Sorption and Reduction Kinetics on the Magnetite (111) Surface. *Environ. Sci. Technol.* **2012**, *46* (7), 3821–3830.

(3) McCormick, M. L.; Adriaens, P. Carbon Tetrachloride Transformation on the Surface of Nanoscale Biogenic Magnetite Particles. *Environ. Sci. Technol.* **2004**, *38* (4), 1045–1053.

(4) Gregory, K. B.; Larese-Casanova, P.; Parkin, G. F.; Scherer, M. M. Abiotic Transformation of Hexahydro-1,3,5-trinitro-1,3,5-triazine by FeII Bound to Magnetite. *Environ. Sci. Technol.* **2004**, *38* (5), 1408–1414.

(5) Gorski, C. A.; Scherer, M. M. Influence of Magnetite Stoichiometry on Fe^{II} Uptake and Nitrobenzene Reduction. *Environ. Sci. Technol.* **2009**, *43* (10), 3675–3680.

(6) Gorski, C. A.; Nurmi, J. T.; Tratnyek, P. G.; Hofstetter, T. B.; Scherer, M. M. Redox Behavior of Magnetite: Implications for Contaminant Reduction. *Environ. Sci. Technol.* **2010**, *44* (1), 55–60.

(7) Klausen, J.; Troeber, S. P.; Haderlein, S. B.; Schwarzenbach, R. P. Reduction of Substituted Nitrobenzenes by Fe(II) in Aqueous Mineral Suspensions. *Environ. Sci. Technol.* **1995**, *29* (9), 2396–2404.

(8) Scheinost, A. C.; Charlet, L. Selenite Reduction by Mackinawite, Magnetite and Siderite: XAS Characterization of Nanosized Redox Products. *Environ. Sci. Technol.* **2008**, *42* (6), 1984–1989.

(9) Missana, T.; Alonso, U.; Scheinost, A. C.; Granizo, N.; García-Gutiérrez, M. Selenite retention by nanocrystalline magnetite: Role of adsorption, reduction and dissolution/co-precipitation processes. *Geochim. Cosmochim. Acta* **2009**, *73* (20), 6205–6217.

(10) Huber, F.; Schild, D.; Vitova, T.; Rothe, J.; Kirsch, R.; Schäfer, T. U(VI) removal kinetics in presence of synthetic magnetite nanoparticles. *Geochim. Cosmochim. Acta* **2012**, *96*, 154–173.

(11) Latta, D. E.; Gorski, C. A.; Boyanov, M. I.; O'Loughlin, E. J.; Kemner, K. M.; Scherer, M. M. Influence of Magnetite Stoichiometry on UVI Reduction. *Environ. Sci. Technol.* **2012**, *46* (2), 778–786.

(12) Giraldo, L.; Erto, A.; Moreno-Piraján, J. C. Magnetite nanoparticles for removal of heavy metals from aqueous solutions: synthesis and characterization. *Adsorption* **2013**, *19* (2–4), 465–474.

(13) Catalette, H.; Dumonceau, J.; Ollar, P. Sorption of cesium, barium and europium on magnetite. *J. Contam. Hydrol.* **1998**, *35* (1–3), 151–159.

(14) Daou, T. J.; Begin-Colin, S.; Grenèche, J. M.; Thomas, F.; Derory, A.; Bernhardt, P.; Legaré, P.; Pourroy, G. Phosphate Adsorption Properties of Magnetite-Based Nanoparticles. *Chem. Mater.* **2007**, *19* (18), 4494–4505.

(15) Liu, C.-H.; Chuang, Y.-H.; Chen, T.-Y.; Tian, Y.; Li, H.; Wang, M.-K.; Zhang, W. Mechanism of Arsenic Adsorption on Magnetite Nanoparticles from Water: Thermodynamic and Spectroscopic Studies. *Environ. Sci. Technol.* **2015**, *49* (13), 7726–7734.

(16) Tombácz, E.; Tóth, I. Y.; Nesztor, D.; Illés, E.; Hajdú, A.; Szekeres, M.; L.Vékás. Adsorption of organic acids on magnetite nanoparticles, pH-dependent colloidal stability and salt tolerance. *Colloids Surf. Physicochem. Eng. Asp.* **2013**, *435*, 91–96.

(17) Heberer, T. Occurrence, fate, and removal of pharmaceutical residues in the aquatic environment: a review of recent research data. *Toxicol. Lett.* **2002**, *131* (1–2), 5–17.

(18) Fatta-Kassinos, D.; Meric, S.; Nikolaou, A. Pharmaceutical residues in environmental waters and wastewater: current state of knowledge and future research. *Anal. Bioanal. Chem.* **2011**, *399* (1), 251–275.

(19) Gothwal, R.; Shashidhar, T. Antibiotic Pollution in the Environment: A Review. *CLEAN – Soil Air Water* **2015**, *43* (4), 479–489.

(20) Fortune, W. B.; Mellon, M. G. Determination of Iron with o-Phenanthroline: A Spectrophotometric Study. *Ind. Eng. Chem. Anal. Ed.* **1938**, *10* (2), 60–64.

(21) Mullin, J. B.; Riley, J. P. The colorimetric determination of silicate with special reference to sea and natural waters. *Anal. Chim. Acta* **1955**, *12*, 162–176.

(22) Parkhurst, D. L.; Appelo, C. A. J. *User's guide to PHREEQC (Version 2) : a computer program for speciation, batch-reaction, one-dimensional transport, and inverse geochemical calculations*; Water-Resources Investigations Report; USGS Numbered Series 99–4259; Water-resources Investigation Report 99–4259. USGS, Denver, Colorado., 1999; p (p. 312).

(23) Ross, D. L.; Riley, C. M. Aqueous solubilities of some variously substituted quinolone antimicrobials. *Int. J. Pharm.* **1990**, *63* (3), 237–250.

(24) Vincent, W. R.; Schulman, S. G.; Midgley, J. M.; van Oort, W. J.; Sorel, R. H. A. Prototropic and metal complexation equilibria of nalidixic acid in the physiological pH region. *Int. J. Pharm.* **1981**, *9* (3), 191–198.

(25) Jolsterå, R.; Gunneriusson, L.; Holmgren, A. Surface complexation modeling of Fe3O4–H+ and Mg(II) sorption onto maghemite and magnetite. *J. Colloid Interface Sci.* **2012**, *386* (1), 260–267.

(26) Marsac, R.; Banik, N. L.; Lützenkirchen, J.; Catrouillet, C.; Marquardt, C. M.; Johannesson, K. H. Modeling metal ion-humic substances complexation in highly saline conditions. *Appl. Geochem.* **2017**, *79*, 52–64.

(27) Paul, T.; Liu, J.; Machesky, M. L.; Strathmann, T. J. Adsorption of zwitterionic fluoroquinolone antibacterials to goethite: A charge distribution-multisite complexation model. *J. Colloid Interface Sci.* **2014**, *428*, 63–72.

(28) Usman, M.; Martin, S.; Cimetière, N.; Giraudet, S.; Chatain, V.; Hanna, K. Sorption of nalidixic acid onto micrometric and nanometric magnetites: Experimental study and modeling. *Appl. Surf. Sci.* **2014**, *299*, 136–145.

(29) Marsac, R.; Martin, S.; Boily, J.-F.; Hanna, K. Oxolinic Acid Binding at Goethite and Akaganéite Surfaces: Experimental Study and Modeling. *Environ. Sci. Technol.* **2016**, *50* (2), 660–668.

(30) Hanna, K.; Boily, J.-F. Sorption of Two Naphthoic Acids to Goethite Surface under Flow through Conditions. *Environ. Sci. Technol.* **2010**, *44* (23), 8863–8869.

(31) Rusch, B.; Hanna, K.; Humbert, B. Sorption and Transport of Salicylate in a Porous Heterogeneous Medium of Silica Quartz and Goethite. *Environ. Sci. Technol.* **2010**, *44* (7), 2447–2453.

(32) Jolivet, J.-P.; Tronc, E. Interfacial electron transfer in colloidal spinel iron oxide. Conversion of Fe3O4-γFe2O3 in aqueous medium. *J. Colloid Interface Sci.* **1988**, *125* (2), 688–701.

(33) White, A. F.; Peterson, M. L.; Hochella, M. F. Electrochemistry and dissolution kinetics of magnetite and ilmenite. *Geochim. Cosmochim. Acta* **1994**, *58* (8), 1859–1875.

(34) Fein, J. B. The effects of ternary surface complexes on the adsorption of metal cations and organic acids onto mineral surfaces. In: R. Hellmann and S.A. Wood (Editors), Water-Rock Interactions, Ore Deposits, and Environmental Geochemistry: A Tribute to David A. Crerar. Geochemical Society, Special Pub. 7, p. 365–378.

(35) Stumm, W.; Morgan, J. J. *Aquatic Chemistry: Chemical Equilibria and Rates in Natural Waters, 3rd ed*, John Wiley & Sons, Inc., New York.; 1996.

(36) Irving, H.; Williams, R. J. P. The stability of transition-metal complexes. *J. Chem. Soc. Resumed* **1953**, *0* (0), 3192–3210.

(37) Timmers, K.; Sternglanz, R. Ionization and divalent cation dissociation constants of nalidixic and oxolinic acids. *Bioinorg. Chem.* **1978**, *9* (2), 145–155.

(38) Xu, J.; Marsac, R.; Wei, C.; Wu, F.; Boily, J.-F.; Hanna, K. Co-binding of Pharmaceutical Compounds at Mineral Surfaces: Mechanistic Modeling of Binding and Cobinding of Nalidixic Acid and Niflumic Acid at Goethite Surfaces. *Environ. Sci. Technol.* **2017**, *51* (20), 11617–11624.

(39) Xu, J.; Marsac, R.; Costa, D.; Cheng, W.; Wu, F.; Boily, J.-F.; Hanna, K. Co-Binding of Pharmaceutical Compounds at Mineral Surfaces: Molecular Investigations of Dimer Formation at Goethite/Water Interfaces. *Environ. Sci. Technol.* **2017**, *51* (15), 8343–8349.

(40) Haggstrom, L.; Annersten, H.; Ericsson, T.; Wappling, R.; Karner, W.; Bjarman, S. Magnetic Dipolar and Electric Quadrupolar Effects on Mossbauer-Spectra. *Hyperfine Interact.* **1978**, *5* (3), 201–214.

(41) Vandenberghe, R. E.; Hus, J. J.; Grave, E. D. Evidence from Mössbauer spectroscopy of neo-formation of magnetite/maghemite in the soils of loess/paleosol sequences in China. *Hyperfine Interact.* **1998**, *117* (1–4), 359–369.

(42) Aristilde, L.; Sposito, G. Complexes of the antimicrobial ciprofloxacin with soil, peat, and aquatic humic substances. *Environ. Toxicol. Chem.* **2013**, *32* (7), 1467–1478.

443 ## Figure captions

444 **Figure 1.** (a) NA adsorption data versus pH for 50 m^2 L^{-1} suspensions of M0.24, M0.33,
445 M0.40, M0.42, M0.44, M0.5 and Fe(II)-amended M0.40 and M0.42 versus pH in a 10 mM
446 NaCl + 20 μM NA solution, after 24h reaction time. Lines correspond to surface
447 complexation modeling results (see text for more details). (b) Final Fe(II) aqueous
448 concentration ($[Fe(II)]_{aq}$) and (c) calculated $(Fe(II)/Fe(III))_{bound}$ in the corresponding
449 experiments. The same legend is used in (a), (b) and (c). The same color is used for
450 experiments conducted with the same total Fe(II)/Fe(III) ratio.

451 **Figure 2.** (a) Uptake data of 200μM Mn(II), Fe(II) or Ni(II) on M0.40 and (b) corresponding
452 NA adsorption data versus pH. Experimental conditions: 50 m^2 L^{-1} suspensions of magnetite,
453 10 mM NaCl, 20 μM NA, 200μM Mn(II), Fe(II) or Ni(II), 24h reaction time. Negative values
454 for Fe(II) uptake at low pH are due to magnetite dissolution.

455 **Figure 3.** Logarithm of surface complexation constant (log ^{S}K, for NA or FLU) versus
456 $(Fe(II)/Fe(III))_{bound}$ determined at pH $\geq$ 8 (where $(Fe(II)/Fe(III))_{bound}$ is constant). This
457 modeling data was obtained using either a magnetite model (for all data) or maghemite (for
458 $Fe(II)/Fe(III) \leq 0.42$).[25]

459 **Figure 4.** NA adsorption data versus pH for 50 m^2 L^{-1} suspensions of M0.40 and Fe(II)-
460 amended M0.40 in a 10 mM NaCl + 20 μM NA solution, after 24h reaction time, in presence
461 of (a) silicates (100 μM) or (b) HA (10 mg L^{-1}). Empty symbols represent the NA adsorption
462 data without Si or HA.

463

464

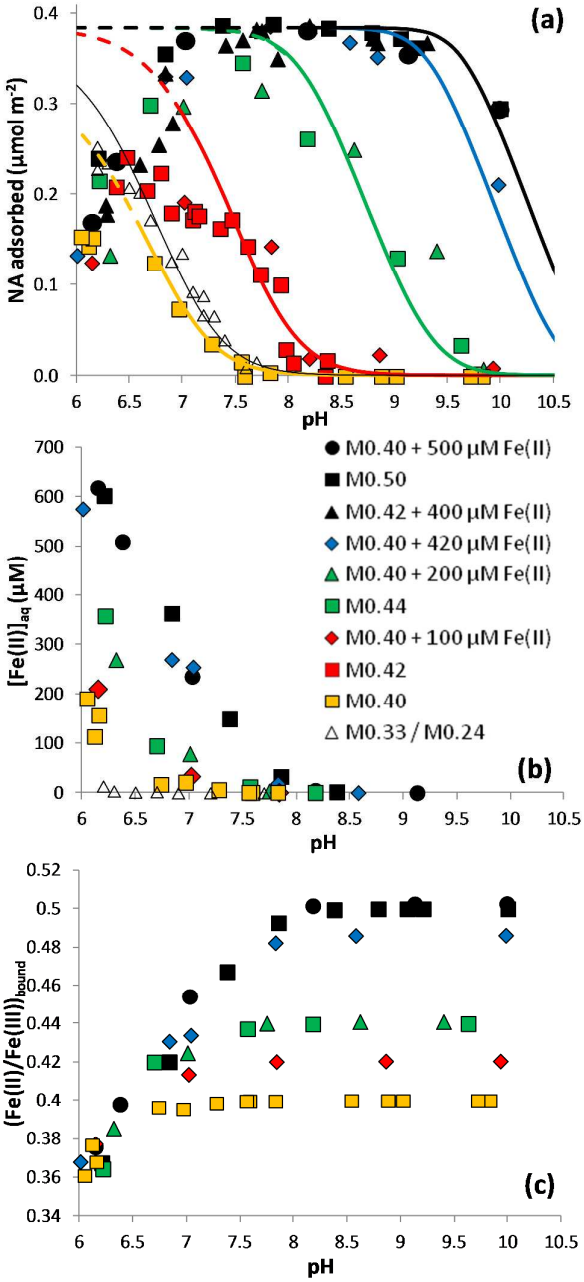

465

466 **Figure 1**

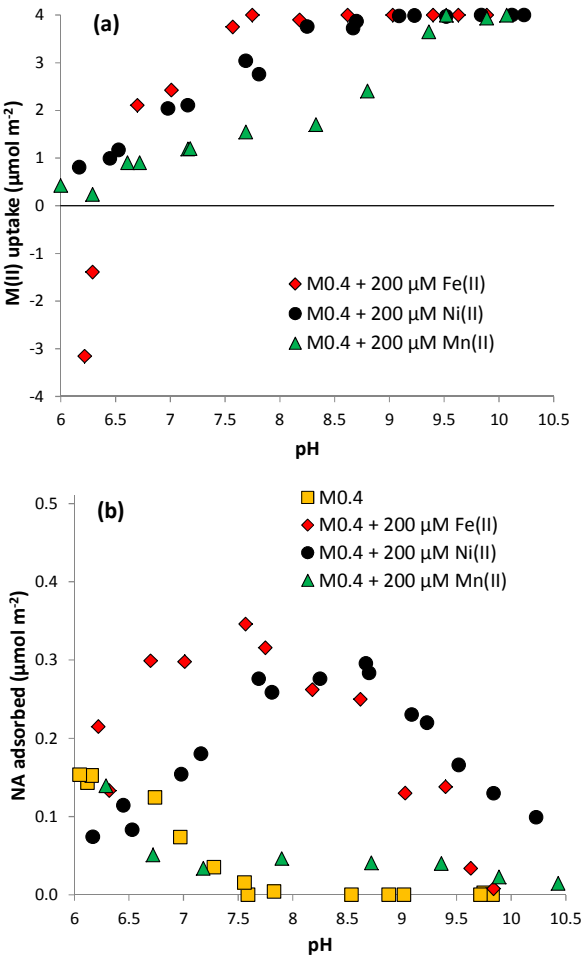

467

468 **Figure 2**

469

470

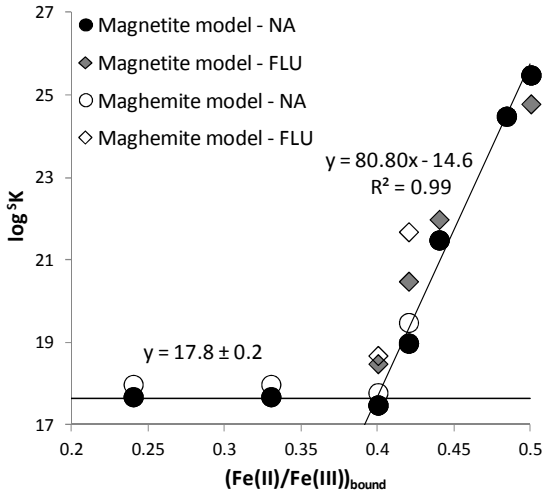

471

472 **Figure 3**

473

474

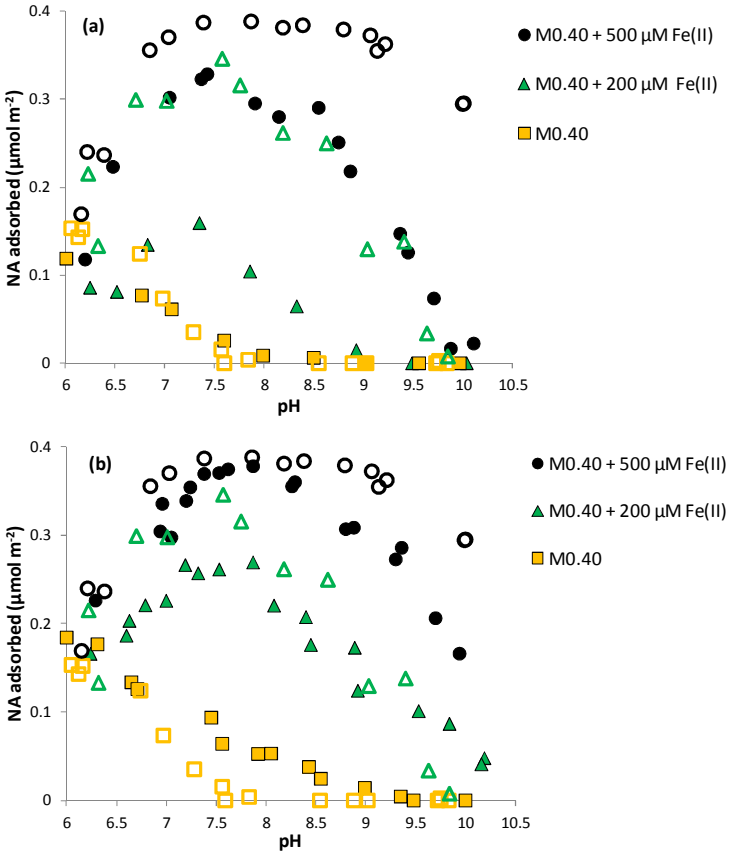

475

476

477 **Figure 4**

478

479

TOC

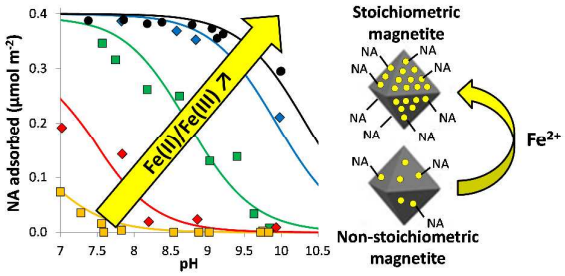

480

481

482

483